Archives of Materials Science and Engineering
Volume 33
Issue 1
September 2008
Pages 21-28
International Scientific Journal published monthly by the World Academy of Materials and Manufacturing Engineering

Crystallographic conditions for the initiation of cavitation erosion in CuMn11Al11 bronze

J. Chmiel [a,*], D. Zasada [b]
[a] Maritime University, ul. Wały Chrobrego 1-2, 70-500 Szczecin, Poland
[b] Military University of Technology, ul. Gen. S. Kaliskiego 2, 00-908 Warszawa, Poland
* Corresponding author: E-mail address: jlc@am.szczecin.pl

Received 24.04.2008; published in revised form 01.09.2008

ABSTRACT

Purpose: The basic aim of this paper is to examine and present specific destruction processes connected with cavitation erosion of multi-component Cu-Mn-Al bronzes. In technical operational conditions these processes are 'masked' by the effects of electrochemical corrosion phenomena. However, these destructive processes may significantly accelerate the destruction of flow devices and marine propulsion systems. The essential phenomena occurring during these processes are incubation and propagation of brittle cracks in the planes of cleavage planes of the ordered phase β (Cu_3Mn_2Al) that occurs in the examined group of alloys. Additional purpose is the assessment of possible applications of alloys with single-phase structure of intermetallic phases as model materials for research into erosion-cavitation resistance.

Design/methodology/approach: This work presents research results concerning erosion cavitation resistance of a model alloy examined at a cavitation jet stand. The destructed areas were examined by gravimetric methods and those using scanning microscopy combined with computer image analysis. As the test materials used were single phase model alloys with the composition simulating selected phase components of Cu-Mn-Al bronzes, it was possible to examine erosion cavitation phenomena in the conditions of minimized effect of electrochemical phenomena.

Findings: It has been found that at the initial period of destruction of the phase β in multi-component Mn-Al bronzes the prevailing form of destruction was a classical attack along grain boundaries, starting from the grain boundary junctions while in cases where the Cu_3Mn_2Al superstructure was present, the major mechanism of the incubation of erosion cavitation damage in the phase β is brittle cracking along cleavage planes {001} oriented at 45° angle to the exposed surface.

Research limitations/implications: An essential problem is the verification of the results obtained using the computer-based image analysis by other methods. It seems purposeful to carry out micro-diffraction examination by the EBSP method and making a 'map' of lattice orientation of particular grains on the surface of a specimen, followed by a series of cavitation tests.

Practical implications: The observed phenomena can be regarded as the basic explanation of observed accelerated wear of marine propellers that had been repaired by casting and welding methods.

Originality/value: The value of this work is that cavitation erosion was examined in the conditions of minimized influence of electrochemical factors.

Keywords: Cavitation erosion; Brittle cracking; Intermetallic alloys; Image analysis

PROPERTIES

1. Introduction

The phenomenon of cavitation is connected with gradients of pressure formed in a liquid and is a consequence of turbulent flow or high power vibrations induced by an external factor. The nature of cavitation and methods of its examination have been described in numerous publications, e.g. [1-3]. The research into cavitation phenomena can be done at various kinds of test stands [3-5]. These stands are mostly adjusted to the specific character of research conducted by particular research teams. The most common type of test stands are vibration stands, both piezoelectric or magnetostrictive units inducing wave cavitation [6-8] or a variety of flow stands where hydrodynamic cavitation can be generated [3, 5, 9]. The most comprehensive overview and comparison of various stand types is included in the report of the International Cavitation Erosion Test (ICET) coordinated by Dr J. Steller of the Institute of Flow Machines, Polish Academy of Sciences [10]. Well recognized standard methods of examining cavitation erosion those using vibratory apparatus as specified in the ASTM G32 - 03 standard as well as the Lichtarowicz's cavitating liquid jet method included in ASTM G134 – 95 (2001) standard.

Cavitation, or cavitation erosion, damages surfaces of hydraulic equipment, washed by fast flowing liquids or working in the area of mechanical vibrations. Such machines or their elements include water turbines, rotodynamic pumps, steam turbines, ship’s propellers, cylinder liners of liquid-cooled engines. Pressure micro- and macro-impulses and microjets of a dynamically flowing liquid are destructive for surfaces of above mentioned flow machines or installations [11-13]. The determination of the correlation between cavitation resistance of materials and their other properties is relatively difficult. There are no universal criteria for the assessment of cavitation resistance based on other properties of these materials [4, 14]. One interesting concept is the so called fractional cavitation erosion resistance in which the destruction process is related to the energy load distribution [3].

Conventional methods of cavitation erosion assessment include:

- gravimetric examination,
- profilographometric examination of the eroded surface,
- light and electron microscopic examination.

Microscopic methods are very often supported by computer-based processing and analysis of the image. Counting and measurements of cavitation losses and the examination of their correlation with cavitation loads are described by Momma and Lichtarowicz [15], Szkodo [26] and other authors. The application of computer image analysis allows to obtain significantly broader information on the conditions and the course of cavitation destruction, in particular it allows to:

- assess the cavitation load distribution on a specimen surface or tested component; this is particularly important when material resistance is examined at test stands inducing a cavitation cloud with a wide energy spectrum and varied geometry;
- assess the orientation of crystallographic network of grains being destroyed on the basis of geometric measurements of losses at initial stages of incubation of cavitation erosion;
- assess the real area subject to erosion in a given stage of the process; this allows to calculate an approximate depth of losses, which is important from the point of view of microturbulence generation on surface imperfections [16].

2. Test stand and research conditions

The test stand existing at the Maritime University of Szczecin is a stand modelling conditions of hydrodynamic cavitation (Fig. 1). The cavitation cloud is generated in a jet of a liquid flowing out of a nozzle and hitting the surface of a specimen rotating on the rotor arm. The characteristic features of the stand are non-homogenous distribution of loads in the jet coming out of the nozzle and a wide energy spectrum of generated cavitation loads [5].

The test stand had the following working parameters during the examinations:

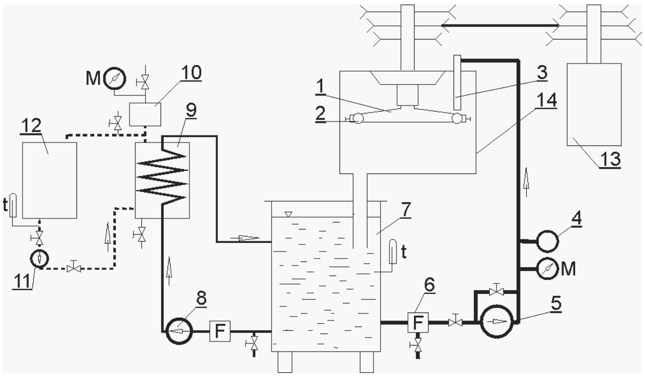

Fig. 1. Diagram of a cavitation jet stand [5]

1-rotor, 2-specimen, 3-nozzle, 4-flowmeter, 5- rotodynamic pump, 6- self-cleaning filter, 7- circulation tank, 8-cooling system pump, 9-cooler, 10- equalizing tank, 11-coolant pump, 12-air cooling unit, 13-electric motor, 14-rotor casing

rotor revolutions	2830 rev/ min
specimen linear velocity	50 m/s
nozzle diameter	6 mm
jet overpressure	0.6 bar
specimen to nozzle face distance	1.6 mm
total exposure time	6 five hour cycles
water temperature	28 ± 5 ° C

Tap water has been used for tests.

3. Research material

Multicomponent Cu-Mn-Al bronzes, also containing Fe and Ni, are basic materials used for the construction of flow equipment, particularly marine propellers and thrusters [17].

Structural components of these bronzes are two solid solutions - α based on Cu and β based on the phase Cu_3Al and a group of intermetallic phases κ having dendritic or globular morphology based on the Fe-Al system. The specific quality of these alloys is their substantial resistance to cavitation erosion; this resistance grows in proportion to the volume share of the phase β [18].

As these alloys have a multiphase structure, they make up complex electrochemical systems, with numerous anode and cathode reactions between alloy phase components. In operational conditions and during standard erosion-cavitation tests these reactions essentially affect the results of the destruction process. The research included the performance of cavitation resistance tests aimed at finding out the behaviour of phase β in conditions of minimum corrosion agents.

The composition of the model alloy used for tests was based on the results of X-ray microanalysis of alloys of the examined group in various technological conditions. The composition of the alloy was specially selected to obtain single phase β type structure with A2 (RPC) lattice. The nominal alloy composition was chosen to be CuAl11Mn11. At a slow cooling speed in the one phase β range, the order observed in the alloy led to the formation of Heusler's superlattice Cu_3Mn_2Al. Fast cooling, in turn, results in supercooled phase β^* [1][17, 18]. These changes correspond to the behaviour of phase β in multi-component manganese-aluminium bronzes, described in the literature on the subject.

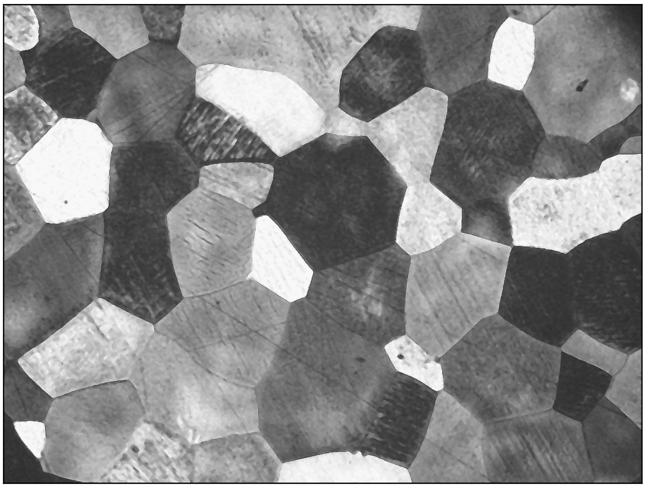

Fig. 2. Microstructure of the model alloy CuMn11Al11. Magnified x 50, etching 10% $(NH_4)_2S_2O_8$

The alloy was tested in the following technological conditions:

- homogenized chill cast, chilled with the furnace (slow cooling conditions), modelling the conditions of cooling in thick-walled parts of a cast;
- cast subject to additional thermal treatment 600°/30 min/water (quenching conditions), modelling the cooling conditions of surface layers.

Preliminary microscopic examinations showed that samples have homogenous, coarse-grained one-phase constitution (Fig. 2).

The samples of two types, treated at the cavitation stand, were examined by two methods, namely light microscopy and scanning electron microscopy.

4. Analysis of test results

During the examination of initial wear stages two characteristic morphological forms of specimen damage effects were observed, different for each technological condition [19].

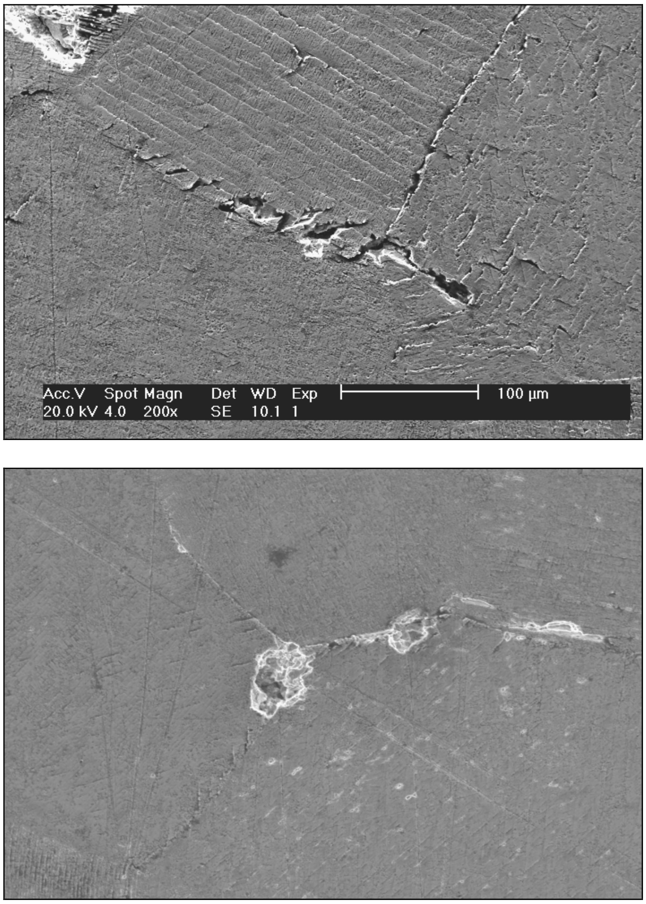

Fig. 3. Damage incubation at the grain boundary. Bronze CuMn11Al11 (SEM)

Form one. After rapid cooling, in the specimens where superstructure did not occur, damage was found to start at a grain boundary interface, and to continue along the boundaries, at spots commencing grain damage (Fig. 3). The arrangement and

---

1 The notation β^* is used, among others, in Brezina's work [18] as a collective notation of supercooled phase β and products of its changes occurring in lower temperatures

concentration of damage at grain boundaries suggested a clear relation to the distribution of cavitation loads. However, the locations of grains that were damaged in the first place did not show such a relation. This form of damage is also observed in intermetallic alloys of the Fe-Al system [20]; in the professional literature it is described as basic in the stage of cavitation erosion incubation in other metallic materials [3, 4, 14].

Form two: In specimens after slow cooling with superstructure present triangular losses were observed to form (Fig. 4a), with morphology similar to that of etching pits, whereas damage occurred only in certain grains. The orientation of triangles was characteristic and approximately the same for each grain damaged. It was found that there exists no clear relation between cavitation loads (changing due to the properties of the test stand used) and the location of grains in which damage was observed (Fig. 4b). Besides, the initiation of damage was not affected by material defects (Fig. 5). Preliminary electron microscopic observations made with the use of an adjustable table allowed to ascertain that facets at the losses are perpendicular to each other (Fig. 6). The analysis of damage morphology of type two makes possible a hypothesis that the critical factor affecting the incubation and propagation of damage in phase β grains is the orientation of the crystallographic lattice of the grains damaged relative to specimen surface [19].

For the verification of the above thesis the following were performed:

- analysis of images previously recorded in the research by SEM and light microscopy as well as analytical calculations of lattice orientation and angles of planes inclination;
- direct measurements of angles during electron microscopic examination.

The following assumptions were made:

- observed planes of facets correspond to cleavage planes {001}, typical of the A2 type lattices and are perpendicular to each other [21] (Fig. 7);
- the specimen surface is a plane described by the equation

$$\frac{x}{x_0} + \frac{y}{y_0} + \frac{z}{z_0} = 1 \tag{1}$$

The dihedral angles α, β and γ between the plane ABC and planes {001} BCD, ACD and ABD were taken as parameters describing the lattice orientation. Having accounted for zero terms for the planes {001} and after the transformation of the ABC plane equation from its section form, we obtain:

$$\begin{aligned}
\cos\alpha &= \frac{y_0 z_0}{\sqrt{(x_0^2 y_0^2 + x_0^2 z_0^2 + y_0^2 z_0^2)}} \\
\cos\beta &= \frac{x_0 z_0}{\sqrt{(x_0^2 y_0^2 + x_0^2 z_0^2 + y_0^2 z_0^2)}} \\
\cos\gamma &= \frac{x_0 y_0}{\sqrt{(x_0^2 y_0^2 + x_0^2 z_0^2 + y_0^2 z_0^2)}}
\end{aligned} \tag{2}$$

where x_0, y_0 and z_0 are solutions to the following system of equations

$$\begin{aligned}
x_0^2 + y_0^2 &= c^2 \\
x_0^2 + z_0^2 &= b^2 \\
y_0^2 + z_0^2 &= a^2
\end{aligned} \tag{3}$$

in which *a*, *b*, *c* are, respectively, lengths of the sections BC, AC and AB [22]. These lengths are obtained directly from measurements of a microscopic image.

a)

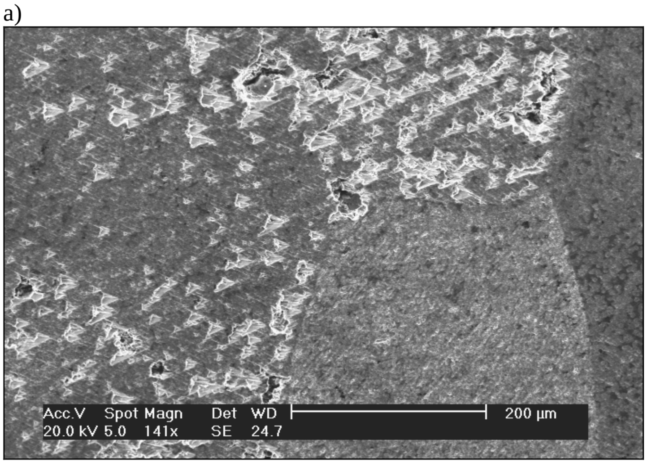

b)

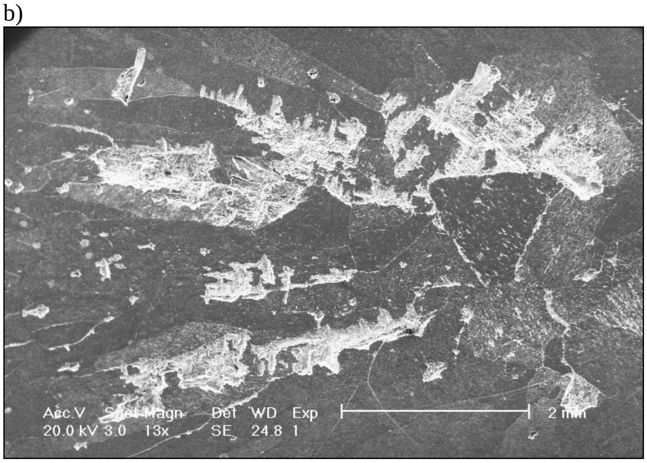

Fig. 4. Morphology of cavitation damage in the model alloy CuMn11Al11 with the superstructure present (SEM);) no damage at grain boundaries, b) selective damage of grains

Therefore, if we know the coordinates of points A,B,C and the distances *a*, *b*, *c* between them, we can calculate all necessary angle parameters of the type two losses. Using practically any computer system of image analysis, the determination of points' coordinates and their entry into a relevant computing procedure is not a troublesome task. In practice, the determination of vertex positions can be done in two ways:

- interactively in any graphic program, returning the coordinate values of a point indicated by the operator;
- automatically, by implementing the procedure including e.g. filtration and binarization of an image, the determination of the skeletons of triangular loss images and the determination of the coordinates of skeleton end branches [23].

The orientations of cleavage planes were experimentally determined in the model alloy specimens that were damaged according to the type two mechanism. The analysis included images from both light and scanning microscopes. The determined values of vertex coordinates were used for calculating the values a, b, c, x_0, y_0, z_0 and relevant cosines of angles between the planes. Twenty to thirty sets of losses were measured from each grain, in which type two damage was observed. Preliminary analysis of data led to a conclusion that two characteristic groups of losses can be classed:

- "triangular" losses, to which cyclically variable values of angles α, β and γ correspond, having, respectively, approximate values of 45°, 60° and 60° (Fig. 8a);
- "elongated" losses, in which two angles are close to 45°, while the third one asymptotically tends to 90° (Fig. 8b).

An extreme case of an elongated loss, defined as a prismatic loss, with two facets inclined at 45° angle, was observed in specimens in which the damage propagated from the grain boundary or from deliberately evoked surface damage (Fig. 9).

The results were confirmed during direct measurements of plane inclination angles performed with a scanning microscope equipped with an adjustable table (Fig. 6). The characteristic phenomena are incubation and propagation of fractures in planes positioned at 45° angle to the plane of specimen surface.

This phenomenon was described by Okada and others who performed cavitation tests of single crystal specimens at a vibration stand [24].

Besides, as it was proved in the work [20], damage of specimens in which superstructure occurred, expressed by loss of mass, ran much more intensively than in specimens with the β* structure.

As it was observed that the standard deviation of calculated angle values heavily depends on the size of image depicting a loss being measured, that parameter was examined for its influence on the uncertainty of the values of cleavage plane inclination angle cosine and on estimated inclination angle values.

The results, calculated using the relation for a multi-variable function uncertainty, given in [25], were computed by means of the Matlab software. It was found that the cleavage plane inclination cosine values are burdened with a relatively small error 5% (0.025 while the mean cosine function equaled 0.5) when the length of loss side observed in a digital image was about100 pixels. For a traingle side length of approximately 100 pixels the probable error of angle estimation was about 2° and it should be considered as satisfactory when the sample size is large enough. Besides, Figure 10 shows that estimated values of cleavage plane inclination angles, obtained at the side length of a triangle formed by the loss image, smaller than 20 pixels should be regarded as at least doubtful. In an extreme case a conclusion can be drawn that the mean value of cleavage plane inclination

Fig. 5. Material defects close to grain boundaries with favourably-oriented crystallographic lattice. No traces of cavitation erosion after 30 hour exposure (SEM)

a)

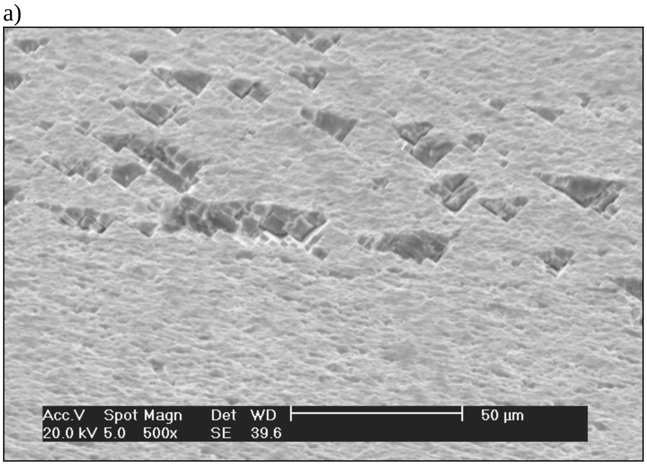

b)

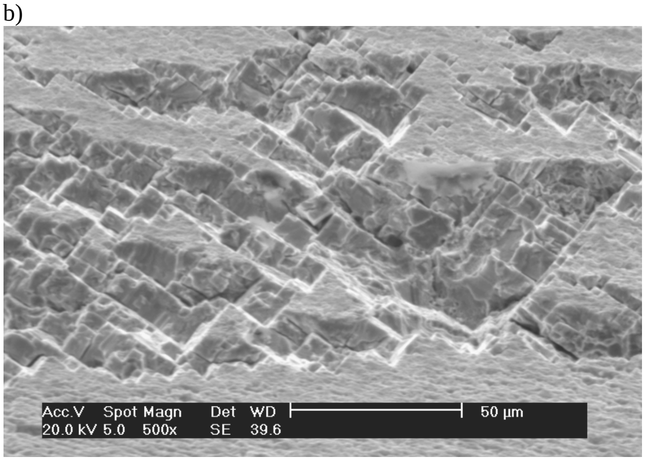

Fig. 6. Perpendicularity of loss facets, visible when the specimen is tilted at 60° angle, initial (a) and advanced stage (b) (SEM)

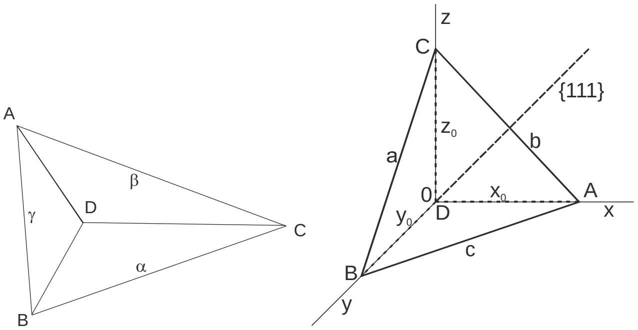

Fig. 7. A diagram of a loss and assumed coordinate system α, β, γ - dihedral angles between facet planes and the microsection plane (specimen)

a)

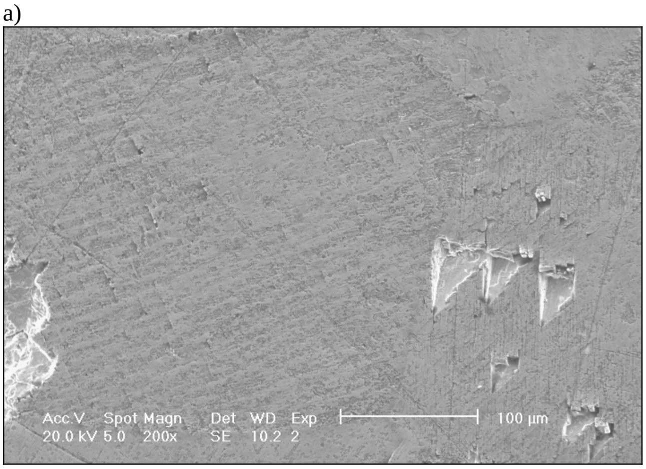

b)

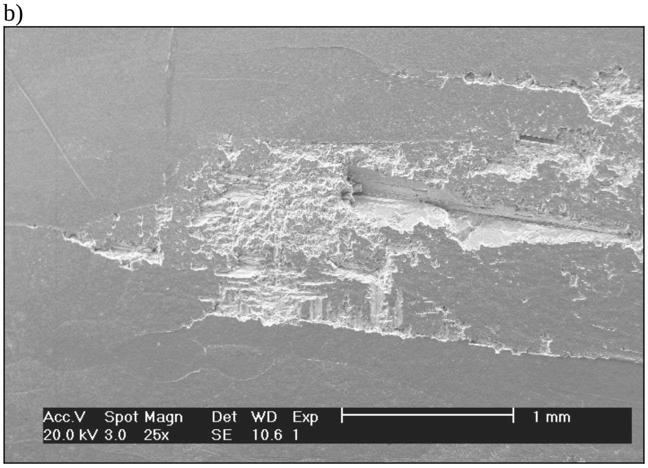

Fig. 8. Characteristic classes of losses in the bronze CuMn11Al11 a) "triangular" losses, b) "elongated" losses (SEM)

angles amounts to about 54°, which approximately corresponds to the perpendicularity of the straight line <111> specimen surface. Therefore, the optical-electronic magnification of an image should be selected so that the size of examined losses, defined with the length of the shortest side, is contained in the optimal range. In addition, it should be noted that while determining angle parameters which was the case here, linear scaling of an image (eg. pixels/ micrometer) is a secondary matter.

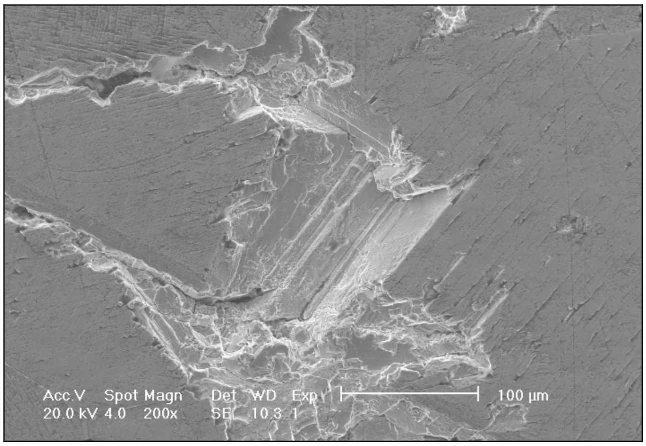

Fig. 9. Prismatic loss with facets inclined at 45° angle. Bronze CuMn11Al11, (SEM)

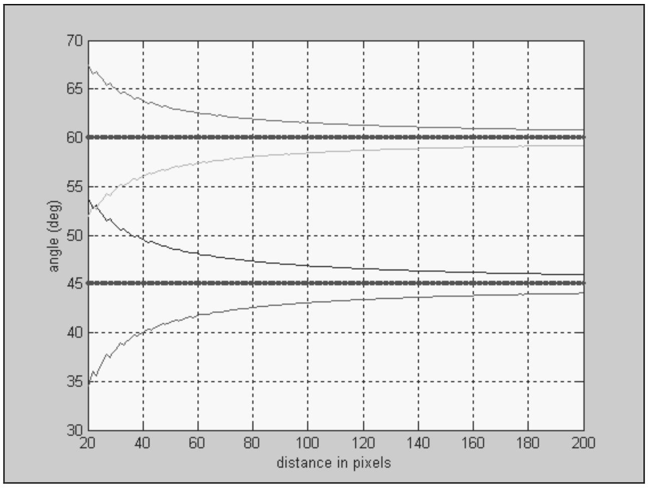

Fig. 10. Uncertainty of cleavage plane inclination angle estimation dependent on side lengths (pixels) for the inclination angles of 45° and 60°

It is also essential to verify the results from computer analysis of an image by other methods. The performance of microdiffraction tests by the EBSP method seems to be more relevant (appropriate). It was found that the microdiffraction image obtained after an exposure of specimens to cavitation, due to substantial pressures and deformations of the surface layer is unreadable and the determination of crystal lattice orientation in particular grains is not possible. Therefore, the following procedure is proposed:

- preparation of specimen surface such that internal pressures are minimized,
- determination of the coordinate system and plotting markers on the specimen surface,
- making a 'map' of lattice orientation of particular grains on the specimen surface,
- performing a series of cavitation tests.

5. Conclusions

1. The use of a model alloy having a one-phase type β or β* structure allowed to assess the behaviour of these phases in conditions free from mechanical or electro-chemical influence of the other phases of an industrial alloy.
2. It is possible to assess the crystallographic orientation of grains subjected to cavitation erosion by analyzing images of losses with characteristic morphology, using computer-based methods of image analysis.
3. In the initial stage of phase β damage in multi-component manganese-aluminium bronzes, where there was no Cu_3Mn_2Al superstructure, the prevailing form of damage was a classical attack along grain boundaries starting from boundary intersection points. In industrial Cu-Mn-Al alloys, subjected to erosion cavitation effect in real conditions produced by tap water, this phenomenon is masked by intensive damage of the phase α [27]. It is possible that in the sea water environment corrosion-cavitation damage of phase β is accelerated [14, 19], so that observation of this form of damage is impossible.
4. Where the superstructure Cu_3Mn_2Al is present, the prevailing mechanism of erosion-cavitation damage incubation in the phase β becomes fracturing along cleavage planes {001} positioned at 45° angle to the exposed surface. This mechanism causes more intensive damage than that caused by a typical mechanism of attack along grain boundaries.
5. In commercial conditions, the circumstances favourable for the formation of Cu_3Mn_2Al superstructure occur, for example, during repairs of damaged propeller blades by casting methods. In such conditions the material is substantially overheated and there is a wide coarse-grained zone of heat effect, which in combination with slow cooling may form the mentioned phase. It seems very probable that during erosion cavitation damage of propellers repaired two mechanisms may interact: conventional damage of phase α and accelerated damage of phase β following the mechanism of fracturing along cleavage planes. This explains why propellers in the repaired places undergo accelerated damage [28].

Standards

G32-03 Standard Test Method for Cavitation Erosion Using Vibratory Apparatus.

G134-95 (2001) Standard Test Method for Erosion of Solid Materials by a Cavitating Liquid Jet.

References

[1] R.T. Knapp, J.W. Daily, F.G. Hammit, Cavitation, McGraw – Hill, New York, 1970.

[2] K. Steller, T. Krzysztofowicz, Methods of materials testing endanger on the cavitation process, Scientific Reports of Institute of Flow Machines (Gdańsk) 152/1072/82 (1982) (in Polish).

[3] J. Steller, International cavitation erosion test and quantitative assessment of material resistance to cavitation, Wear 233-235 (1999) 51-64.

[4] J. Hucińska, M. Głowacka, State of examination on the cavitation destruction of alloys metals and the protection. Materials Engineering 2 (2001) 79-86 (in Polish).

[5] R. Jasionowski, Examination of materials resistivity on the cavitation erosion, Scientific Reports WSM Szczecin 72 (2003) 105- 120.

[6] H.M. Shalaby, A. Al-Hashem, H. Al-Mazeedi, A. Abdullah, Field and laboratory study of cavitation corrosion of nickel aluminium bronze in sea water, British Corrosion Journal 30/1 (1995) 63-70.

[7] J.T. Chang, C.H. Yeh, J.L. He, K.C. Chen, Cavitation erosion and corrosion behavior of Ni-Al intermetallic coatings, Wear 255/1-6 (2003) 162-169.

[8] W.J. Tomlinson, N. Kalitsounakis, G. Vekinis, Cavitation erosion of aluminas, Ceramics International 25/4 (1999) 331-338.

[9] M. Matsumura, K. Noishiki, A. Sakamoto, Jet-in-slit test for reproducing flow-induced localized corrosion on copper alloys, Corrosion 54/1 (1998) 79-88.

[10] ICET transactions, http://www.imp.gda.pl/icet/index.htm

[11] G. Silva, Wear generation in hydraulic pumps, SAE Transactions 99/2 (1990) 635-652.

[12] Grinberg, A. Ya, Consideration of corrosion in material cavitation stability determination, Tyazheloe Mashinostroenie 12 (1992) 15-16 (in Russian).

[13] G. Patience, Developments in marine propellers, Proceedings of the Institution of Mechanical Engineers, Power and Process Engineering A205/2 (1991) 77-88.

[14] J. Chmiel, J. Grabian, Chosen problems of resistivity on the cavitation erosion of multiphase metallic materials, Proceedings of the International Conference „Technology '99”, Bratysława, 1999, 916-920.

[15] T. Momma, A. Lichtarowicz, Study of pressures and erosion produced by collapsing cavitation, Wear 186-187/2 (1995) 425-436.

[16] G.A. Schmitt, W. Buecken, R. Fanebust, Source: Modeling microturbulences at surface imperfections as related to flow-induced localized corrosion, Corrosion 48/5 (1992) 431-440.
[17] A. Kowarsch, Z. Zaczek, Cooper and its alloys in the shipbuilding, Marine Press, Gdańsk, 1989 (in Polish).
[18] P. Brezina, Heat Treatment of Complex Aluminium Bronzes, International Metal Reviews 27/2 (1982) 77-120.
[19] J. Chmiel, D. Zasada, Corrosion-cavitation destruction of β phase in multicomponent manganium-aluminum bronzer, Corrosion protection 11s/A/2003 205-208 (in Polish).
[20] J. Chmiel, R. Jasionowski, W. Przetakiewicz, D. Zasada, Corrosion-cavitation properties of phase components of manganium-aluminum bromzes, Exploitation problems 4/2003 19-28 (in Polish).
[21] J.W. Wyrzykowski, E. Pleszakow, J. Sieniawski, Deformation and cracking of metals, WNT, Warsaw, 1999.
[22] Mathematics – Engineers handbook, WNT, Warsaw, 1986.
[23] L. Wojnar, K.J. Kurzydłowski, J. Szala, Practics of image analysis, Polish Stereological Society, Cracow, 2002.
[24] T. Okada, S. Hattori, F. Suzuki, Fundamental study on cavitation erosion using a magnesium oxide single crystal. Transactions of the Japan Society of Mechanical Engineers A 60/569 (1994) 147-152.
[25] J.R. Taylor, An Introduction to Error Analysis, Oxford University Press, 1982.
[26] M. Szkodo, Application of image analysis methods in the determination of materials' cavitation resistivity, Exploitation Problems 1/2006 (in Polish).
[27] R. Jasionowski, J. Chmiel, D. Zasada, Examination of cavitation resistivity of Cooper alloys applied as a power screw, Proceedings of the 10th Congress "Technical Devices Exploitation", Jabłonki, 2005, 179-188.
[28] L. Wilczyński, Cavitation erosion of screws and rudders, Proceedings of the CTO Seminar, Gdańsk, 2005.